The laboratory millimeter and submillimeter spectrum of HCO[a)]

Geoffrey A. Blake

Department of Chemistry, California Institute of Technology, Pasadena, California 91125

K. V. L. N. Sastry

Department of Physics, University of New Brunswick, Fredericton, New Brunswick, Canada E3B 5A3

Frank C. De Lucia

Department of Physics, Duke University, Durham, North Carolina 27706
(Received 16 June 1983; accepted 12 September 1983)

The rotational absorption frequencies of 68 new lines from the HCO radical in its ground electronic state have been measured in the millimeter and submillimeter spectral region. The large zero-field data set acquired has allowed the complex spectrum of this light asymmetric rotor with unpaired electronic spin and magnetic hyperfine interactions to be completely analyzed to within experimental accuracy (< 0.1 MHz) for the first time. The wide range of states observed provides a highly accurate map of the rotational frequencies of the formyl radical, which should enable the abundance and excitation of interstellar HCO to be examined in detail.

I. INTRODUCTION

The formyl radical HCO is an active participant in a wide variety of chemical processes. For example, HCO is known to be abundant in hydrocarbon flames,[1] and has also been observed in several interstellar molecular clouds.[2,3] In addition, the formyl radical was the first unstable nonlinear free radical detected through its pure rotational spectrum in a zero-field microwave absorption experiment.[4] Several authors[5,6] have therefore used HCO as a testing ground for theoretical interpretations of the rotational spectra of light asymmetric rotors with an unpaired electron spin. In spite of such great interest, experimental observations of the rotational spectrum of the formyl radical have proven to be difficult.

Bowater *et al.*[7] first investigated the pure rotational spectrum of HCO using gas-phase EPR to detect the $2_{11} - 2_{12}$ K-doubling transition near 8.4 GHz. The constants of this work and optical studies[8] enabled Saito[4] to observe the four strongest components of the $1_{01} - 0_{00}$ transition at 86.7 GHz in a zero-field experiment. Pickett and Boyd[9] have also measured this transition by photolyzing mercury sensitized acetaldehyde. The $2_{11} - 2_{12}$ and several other K-doubling transitions within the $N=1$ and $N=3$ rotational levels of the $K_p=1$ stack have also been detected by Austin *et al.*[10] in a lower frequency zero-field study of HCO. The only other $\Delta N=1$ transition frequency reported to date is a measurement of the $8_{26} - 7_{17}$ b-type transition by Cook *et al.*[11] using far infrared laser magnetic resonance. An infrared laser magnetic resonance study of the ν_2 (CO stretch) vibration by Brown *et al.*[12] has also given some information about centrifugal distortion effects in the formyl radical.

None of these studies, however, have produced the extensive data set needed to experimentally determine the large set of molecular constants required to completely fit the rotational spectrum of HCO. This occurs primarily because of the great chemical reactivity of the formyl radical, and because most of its rotational spectrum falls at shorter millimeter and submillimeter wavelengths. The high frequencies of most of the transitions make zero-field experiments difficult, while the rapid uncoupling of the unpaired electron spin from the molecular framework imposes stringent coincidence requirements on magnetic resonance studies. Discussions of the molecular constants, such as that by Boland, Brown, and Carrington,[13,14] have therefore relied on a mix of theoretically and experimentally derived parameters. More recently Brown *et al.* have analyzed a newly acquired set of far-infrared LMR data, which has produced a full set of rotational constants presented in a reanalysis of the infrared LMR data.[15] In this work, we report the measurement of 34 new transitions (all with resolved hyperfine structure) in the frequency range between 140 and 360 GHz, with values of N and K up to 11 and 3. The results reported here include the first zero-field measurements of b-type pure rotational transitions of HCO. The large data set acquired has enabled an extensive set of molecular constants to be determined to microwave accuracy. In addition, the transition frequencies provided by this work should allow for a confirmation and more complete survey of the presence of HCO in the interstellar medium, which currently rests upon the detection of the strongest hyperfine component of the $N=1_{01} - 0_{00}$, $J=3/2 - 1/2$ transition.[2,3]

II. EXPERIMENTAL

The details of our millimeter and submillimeter spectroscopic technique have previously been discussed

[a)]Work supported by: NASA Grant No. NAGW-189.

 0021-9606/84/010095-07$02.10

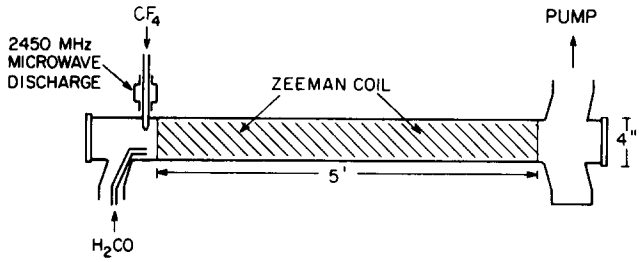

FIG. 1. Free space microwave discharge absorption cell used to produce and study HCO.

elsewhere.[16] Briefly, a reflex klystron operating in the 50 GHz region is used to drive a silicon diode multiplier, the output radiation of which is filtered by step-down waveguide sections to select the appropriate harmonic(s), focused through a free-space absorption cell by quasioptical techniques, and detected by a 1.4 K InSb hot-electron bolometer. A low pressure glow discharge of H_2 and CO failed to produce observable signals from HCO. Therefore, as in previous studies, the formyl radical was produced by the reaction of atomic fluorine with formaldehyde.[4,7] Atomic fluorine was generated by discharging CF_4 at 2450 MHz, while formaldehyde was obtained by heating solid paraformaldehyde to 90 °C. The absorption cell used in the study of HCO is shown in Fig. 1. A compact microwave discharge cavity[17] powered by a 100 W microwave diathermy unit was mounted on a small arm at the head of the cell. A solenoid wrapped around the length of the cell produced a longitudinal magnetic field which was used for Zeeman modulation. Formaldehyde entered the cell through a thin glass pipe whose tip was placed at the end of the microwave discharge tube to insure efficient mixing. A fast flow configuration was maintained by a 4 in. diffusion pump. Produced under a wide range of conditions, maximum HCO absorption signals were observed with an equimolar mixture of H_2CO and CF_4 (measured with the discharge off) at a total pressure of ~30 mTorr with the diffusion pump fully unthrottled.

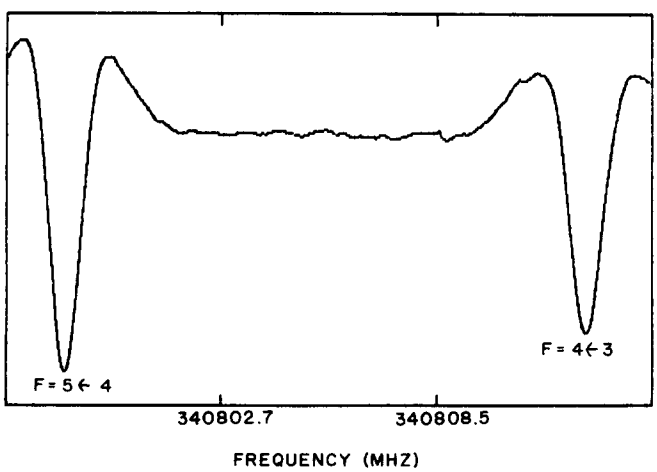

FIG. 2. The $J = 9/2 \leftarrow 7/2$ fine structure component of the $4_{14} \leftarrow 3_{13}$ a-type rotational transition in HCO.

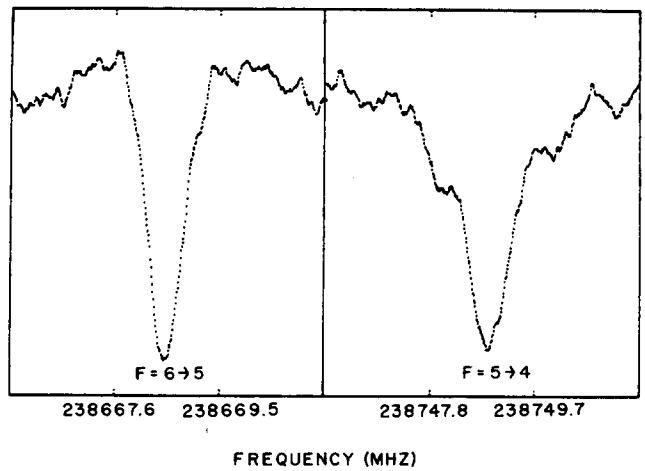

FIG. 3. The $J = 9/2 \leftarrow 11/2$ fine structure component of the $4_{14} \leftarrow 5_{05}$ b-type rotational transition in HCO.

Although stronger transitions of HCO could be observed using video detection, all of the measurements were made with phase-locked klystrons and lock-in detection techniques. Sinusoidal Zeeman modulation at 2.6 kHz and $2f$ signal recovery at 5.2 kHz proved to be the most effective modulation scheme, particularly below 300 GHz where baseline effects can become severe if source modulation is used. Square wave Zeeman modulation was initially used to detect strong a-type lines, but was found to be more susceptible to pickup than sine wave modulation as signal recovery must take place at the modulation frequency. All a-type lines were measured by recording several pairs of 100 s sweeps with a 1 s lock-in time constant on a dual chart recorder, while all b-type lines were collected in a digital signal averager and processed and measured in a computer. The integration times ranged from 3 min (ten up–down sweeps) for strong lines to 30 min (100 up–down sweeps) for the weaker ones. Results from the forward–reverse sweeps were averaged to cancel the time-constant induced shift in the observed line center frequencies. Figures 2 and 3 show typical data. Modulation broadening of the spectral lines was not encountered at the field strengths used ($\lesssim 10$ G).

III. THEORY

HCO is a light, nearly prolate, asymmetric rotor with one unpaired electron and one nonzero nuclear spin. A coupling scheme appropriate for discussions of its rotational spectrum is therefore

$$\mathbf{N} + \mathbf{S} = \mathbf{J} , \tag{1a}$$

$$\mathbf{J} + \mathbf{I} = \mathbf{F} , \tag{1b}$$

where **N** is the rotational angular momentum of the molecular framework, **S** is the electron spin angular momentum, and **I** is the nuclear spin of the hydrogen nucleus. Each rotational level $N_{K_pK_o}$ is split into a doublet by the spin-rotation interaction, the levels of which are further split into doublets by magnetic hyperfine interactions, with the final energy levels labeled by the quantum numbers $F = J \pm 1/2$. The effective zero-field Hamiltonian of HCO may be split into the terms[6]

$$H_{eff} = H_{rot} + H_{cd} + H_{sr} + H_{srcd} + H_{hfs} , \quad (2)$$

where H_{rot} is the rigid asymmetric rotor Hamiltonian, H_{cd} corrects for the rotational centrifugal distortion effects absent in H_{rot}, H_{sr} depicts the electron spin-rotation interaction, H_{srcd} contains the centrifugal distortion corrections to H_{sr}, and H_{hfs} accounts for the magnetic hyperfine interaction between the spins of the unpaired electron and the hydrogen nucleus.

As HCO has been studied by several high resolution techniques (EPR, LMR, lower frequency microwave spectroscopy, etc.) the terms in the above Hamiltonian have been studied by a number of authors. Its spectrum is also similar to that of HO_2 and this analysis of HCO follows closely the analysis of HO_2 by Charo and De Lucia.[18] However, as noted below, there are some significant differences. Watson's A-reduced Hamiltonian has been used for H_{rot} and H_{cd}, as in our previous studies of singlet light asymmetric rotors.[19] The A and S reduced Hamiltonians for H_{sr} and H_{srcd} have been presented by Brown and Sears,[20] who show that only four, not five, quadratic spin-rotation parameters are determinable for molecules with a single plane of symmetry. For consistency with the choice of H_{rot} and H_{cd}, the A reduced forms of H_{sr} and H_{srcd} must be used. In the principal axis system of the molecule, H_{sr} may be written as

$$H_{sr} = \tfrac{1}{2} \sum_{\alpha,\beta} \epsilon_{\alpha\beta} (N_\alpha S_\beta + S_\beta N_\alpha) . \quad (3)$$

Explicit forms of the matrix elements of the effective spin-rotation Hamiltonian have been given by Raynes[21] and Bowater, Brown, and Carrington.[6] In our analysis of HCO, we have found it necessary to add an additional term to H_{srcd}. In our earlier work on HO_2 and NO_2, we found that only terms through K^4 were necessary. However, we have found that for HCO, an additional term of the form

$$\langle NKSJ | H^{(6)}_{srcd} | NKSJ \rangle = H^s_K \left[\frac{J(J+1) - N(N+1) - S(S+1)}{2N(N+1)} \right] K^6 \quad (4)$$

is required.

The magnetic hyperfine Hamiltonian H_{hfs} is simply

$$H_{hfs} = a_H \mathbf{S} \cdot \mathbf{I} + \mathbf{S} \cdot \mathbf{T} \cdot \mathbf{I} , \quad (5)$$

where the first term is the isotropic Fermi contact interaction between the electron and proton spins, while the second term arises from the anisotropic dipolar coupling of these spins.

The coupling scheme of Eq. (1) determines the basis in which the effective Hamiltonian is most nearly diagonal. In the absence of external fields, F is a constant of the motion and therefore no matrix elements off-diagonal in F are present. Thus, a direct approach in which the Hamiltonian matrix is diagonalized after assembling it into blocks with a common value of F could be used. Unfortunately, this approach requires the diagonalization of many matrices with large dimension ($\sim 100 \times 100$). Symmetry principles and approximation methods are therefore employed.

In our earlier HO_2 analysis, the hyperfine Hamiltonian could be separated from the total Hamiltonian and treated by perturbation theory because

$$E_{rot} \gtrsim E_{sr} \gg E_{hfs} . \quad (6)$$

After removing the small hyperfine contributions to the observed transitions, calculation of the asymmetric rotor energy levels including spin rotation was then based on the diagonalization of the Hamiltonian $H_0 = H_{eff} - H_{hfs}$, which is diagonal in J. The eigenvector matrix from this analysis was used to rotate H_{hfs} into the asymmetric rotor basis, wherein the matrix elements of H_{hfs} were calculated to determine the final energy levels. This procedure neglects hyperfine matrix elements off-diagonal in J, which could be handled via second order perturbation theory when necessary (e.g., elements diagonal in N and K for $K = 0$). In HCO, however, the interactions are such that

$$E_{rot} \gg E_{sr} \gtrsim E_{hfs} , \quad (7)$$

and it is difficult to completely separate the hyperfine structure from the total Hamiltonian via perturbation theory. Energy levels with the same value of N and F are coupled and perturbed by magnetic hyperfine matrix elements off-diagonal in J, the perturbation being proportional to

$$\frac{(\text{hyperfine matrix element})^2}{\Delta E} \quad (8)$$

in the second order approximation, where ΔE is the separation of the energy levels. The large value of a_H and the small value of ΔE in HCO create large perturbations and render second order theory inadequate. Figure 4 shows the effects of the hyperfine perturbation on the

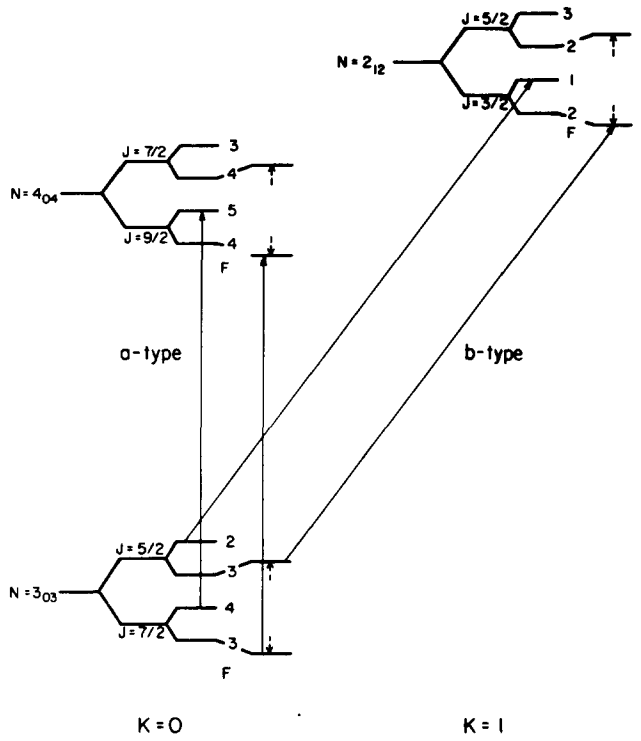

FIG. 4. Illustration of the hyperfine perturbations in HCO on the energy levels of, and transitions from, the $N = 3_{03}$ rotational level.

energy levels of and transitions from the $N=3_{03}$ rotational level. As is clear from the figure for a-type transitions, the perturbed energy levels move in the same direction and the transition frequency is not greatly altered, while for $K_p=0\leftarrow 1$ b-type transitions the perturbations add—creating large shifts of up to 150 MHz. Fortunately, of the four strongly allowed transitions between the fine and hyperfine components of the rotational levels, only two are affected by the large hyperfine perturbation, as Fig. 4 shows. The other two transitions may be treated in an analogous manner to the HO_2 study, and it is this set of data that has been used to calculate the rotation/spin-rotation constants of HCO.

After the hyperfine structure is removed, the remaining J blocks of H_0 have dimensions of $4J+2\times 4J+2$. In order to reduce the problem further, a modified Wang transformation, appropriate for doublet states, is applied to H_0 as suggested by Raynes.[21] This judicious use of symmetry ideally reduces each J block into a set of four submatrices of dimension $J+1/2$. However, for molecules like HCO and HO_2 which lack C_{2v} symmetry, $\epsilon_{ab}+\epsilon_{ba}\neq 0$, and the matrix elements of this part of H_{sr} couple the four submatrices. Perturbation theory is used to include this small effect, with corrections to the transition frequencies arising from ϵ_{ab} inserted before the nonlinear least squares analysis. As Brown and Sears have noted,[20] the values of ϵ_{ab} and ϵ_{ba} are not independent. Therefore, only the matrix elements of ϵ_{ab} were included in the Hamiltonian.

IV. RESULTS AND DISCUSSION

Figure 5 shows an energy level diagram of the HCO molecule and the transitions studied in this work, which are listed in Table I. In all cases, the nuclear hyperfine splittings are easily resolved. As discussed in the previous section, the hyperfine splittings and the rotation/spin rotation structure of the molecule are analyzed separately. First, the observed hyperfine splittings were used to calculate the hyperfine constants a_H, T_{bb}, and T_{cc} in a weighted least squares fit. At higher values of N, it is possible for imprecise knowledge (from the rotation/spin rotation fit) of the energy denominator of Eq. (8) to perturb this calculation. This problem can be eliminated by fitting for the sum of the observed hyperfine splittings in each of the $9_{09}-8_{18}$, $10_{0,10}-9_{19}$, and $11_{0,11}-10_{1,10}$ rotational transitions. Such a procedure cancels any errors that might arise from this source and the 42 measured hyperfine splittings are reduced to 39 independent data points. The constants calculated from the hyperfine analysis are shown in Table III. The rms deviation of the data points taken from Table I is ~0.1 MHz. There is some evidence that this could be reduced further by the inclusion of distortion terms into the hyperfine Hamiltonian, but the small size of these effects would not seem to justify it at present.

The results of this analysis were then used to calculate theoretical line frequencies from which hyperfine contributions had been eliminated. Table II shows these frequencies and Table III presents the spectral

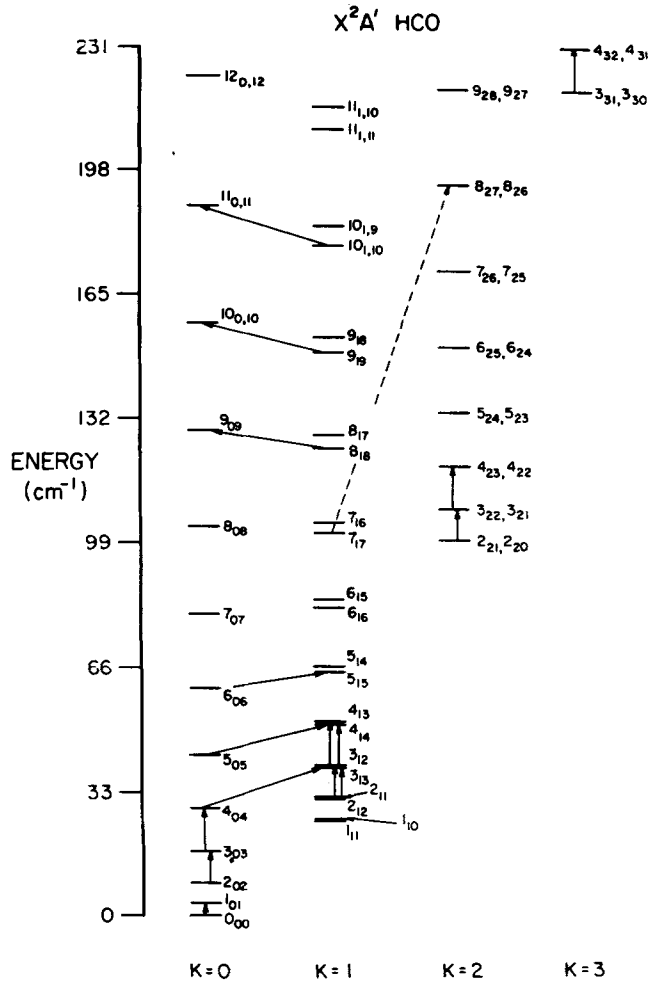

FIG. 5. Energy level diagram of HCO from the constants of this work excluding the fine and hyperfine splittings. Solid arrows indicate the transitions observed in this study.

constants that resulted from the combined rotation/spin rotation and hyperfine fits. The variance of the rotation/spin rotation fit is ~50 kHz. We do not fit directly for A, B, C, ϵ_{aa}, ϵ_{bb}, and ϵ_{cc} but rather linear combinations of these constants. Table IV presents the fitted linear combinations used and their numerical values from which the six rotation/spin rotation constants listed above are calculated. Good statistical redundancy for the calculation of the constants was obtained from the large data set acquired and the results are generally insensitive to the details of the data set or to reasonable selections of terms to be retained in the Hamiltonian.

In addition to our new millimeter and submillimeter observations, we have also included in our weighted analysis the previous microwave data and the LMR measurement by Cook *et al.*[11] of the $8_{26}-7_{17}$ transition. This latter data point is necessary to allow the independent calculation of A and D_K. As a result, the values of these constants depend upon this measurement, while the statistical uncertainty in A and D_K depend upon its reported uncertainty (2 MHz).

A comparison of the derived constants with those previously published is complicated by several factors.

TABLE I. Observed transition frequencies (MHz) of $X\,^2A'$ HCO.

Transition	J	F	Observed frequency (MHz)
$3_{03} \leftarrow 2_{02}$	7/2←5/2	4←3	260 060.329
		3←2	260 082.192
$3_{03} \leftarrow 2_{02}$	5/2←3/2	3←2	260 133.586
		2←1	260 155.769
$3_{13} \leftarrow 2_{12}$	7/2←5/2	4←3	255 341.122
		3←2	255 358.430
$3_{13} \leftarrow 2_{12}$	5/2←3/2	3←2	256 875.347
		2←1	256 892.171
$3_{12} \leftarrow 2_{11}$	7/2←5/2	4←3	263 911.659
		3←2	263 927.215
$3_{12} \leftarrow 2_{11}$	5/2←3/2	3←2	265 334.325
		2←1	265 348.661
$3_{21} \leftarrow 2_{20}$	7/2←5/2	4←3	258 202.056
		3←2	258 216.096
$3_{21} \leftarrow 2_{20}$	5/2←3/2	3←2	264 343.220
		2←1	264 350.121
$3_{22} \leftarrow 2_{21}$	7/2←5/2	4←3	258166.583
		3←2	258180.460
$3_{22} \leftarrow 2_{21}$	5/2←3/2	3←2	264 309.081
		2←1	264 316.003
$4_{04} \leftarrow 3_{03}$	9/2←7/2	5←4	346 708.493
		4←3	346 725.172
$4_{04} \leftarrow 3_{03}$	7/2←5/2	4←3	346 787.898
		3←2	346 804.597
$4_{14} \leftarrow 3_{13}$	9/2←7/2	5←4	340 798.216
		4←3	340 812.078
$4_{14} \leftarrow 3_{13}$	7/2←5/2	4←3	341 671.586
		3←2	341 685.256
$4_{13} \leftarrow 3_{12}$	9/2←7/2	5←4	352 204.257
		4←3	352 214.861
$4_{13} \leftarrow 3_{12}$	7/2←5/2	4←3	352 967.885
		3←2	352 978.060
$4_{22} \leftarrow 3_{21}$	9/2←7/2	5←4	345 743.972
		4←3	345 752.037
$4_{22} \leftarrow 3_{21}$	7/2←5/2	4←3	348 864.210
		3←2	348 870.264
$4_{23} \leftarrow 3_{22}$	9/2←7/2	5←4	345 655.582
		4←3	345 663.584
$4_{23} \leftarrow 3_{22}$	7/2←5/2	4←3	348 778.174
		3←2	348 784.214
$4_3 \leftarrow 3_3$ [a]	9/2←7/2	5←4	344 177.558
		4←3	344 186.067
$4_3 \leftarrow 3_3$ [a]	7/2←5/2	4←3	351 482.848
		3←2	351 485.316
$3_{13} \leftarrow 4_{04}$	5/2←7/2	3←4	328 009.806
		2←3	328 085.568
$3_{13} \leftarrow 4_{04}$	7/2←9/2	4←5	331 180.457
		3←4	331 259.705
$4_{14} \leftarrow 5_{05}$	7/2←9/2	4←5	236 286.654
		3←4	236 363.280
$4_{14} \leftarrow 5_{05}$	9/2←11/2	5←6	238 668.347
		4←5	238 748.777
$5_{15} \leftarrow 6_{06}$	9/2←11/2	5←6	143 080.025
		4←5	143 161.676
$5_{15} \leftarrow 6_{06}$	11/2←13/2	6←7	144 956.679
		5←6	145 042.054
$9_{09} \leftarrow 8_{18}$	17/2←15/2	9←8	143 985.560
		8←7	144 138.270
$9_{09} \leftarrow 8_{18}$	19/2←17/2	10←9	143 191.199
		9←8	143 340.336
$10_{0,10} \leftarrow 9_{19}$	19/2←17/2	10←9	242 117.059
		9←8	242 181.559
$10_{0,10} \leftarrow 9_{19}$	21/2←19/2	11←10	241 420.880
		10←9	241 481.891
$11_{0,11} \leftarrow 10_{1,10}$	21/2←19/2	11←10	341 210.057
		10←9	341 242.607
$11_{0,11} \leftarrow 10_{1,10}$	23/2←21/2	12←11	340 634.955
		11←10	340 664.020

[a] K-type doubling is not resolved.

In large multiparameter fits such as those required for HCO, the correlation among the constants is significant and the contribution of higher order constants to transition frequencies of even low N transitions is important. Thus, lower order constants that were derived[4,7,9,10,13,14] from the few previously available microwave data points

TABLE II. Hyperfine corrected transition frequencies (MHz) used in the rotation/spin-rotation analysis of HCO.

Transition	J	Frequency used in analysis (MHz)	Observed − calculated
$1_{01} \leftarrow 0_{00}$	3/2←1/2	86 671.38[a,b]	0.09
$1_{01} \leftarrow 0_{00}$	1/2←1/2	86 811.35[a,b]	−0.24
$1_{10} \leftarrow 1_{11}$	1/2←1/2	2 726.05[a]	−0.20
$1_{10} \leftarrow 1_{11}$	3/2←3/2	2 890.89[a]	0.07
$2_{11} \leftarrow 2_{12}$	3/2←3/2	8 343.73[a]	1.01
$2_{11} \leftarrow 2_{12}$	5/2←5/2	8 623.22[a]	−0.46
$3_{12} \leftarrow 3_{13}$	5/2←5/2	16 801.01[a]	0.97
$3_{12} \leftarrow 3_{13}$	7/2←7/2	17 194.99[a]	0.92
$3_{03} \leftarrow 2_{02}$	7/2←5/2	260 060.47	−0.04
$3_{03} \leftarrow 2_{02}$	5/2←3/2	260 155.22	−0.04
$3_{13} \leftarrow 2_{12}$	7/2←5/2	255 341.47	0.04
$3_{13} \leftarrow 2_{12}$	5/2←3/2	256 891.86	0.04
$3_{12} \leftarrow 2_{11}$	7/2←5/2	263 911.82	0.00
$3_{12} \leftarrow 2_{11}$	5/2←3/2	265 349.13	−0.03
$3_{12} \leftarrow 2_{20}$	7/2←5/2	258 202.77	−0.03
$3_{21} \leftarrow 2_{20}$	5/2←3/2	264 353.37	−0.04
$3_{22} \leftarrow 2_{21}$	7/2←5/2	258167.30	0.00
$3_{22} \leftarrow 2_{21}$	5/2←3/2	264 319.26	0.05
$4_{04} \leftarrow 3_{03}$	9/2←7/2	346 708.58	−0.05
$4_{04} \leftarrow 3_{03}$	7/2←5/2	346 804.37	−0.01
$4_{14} \leftarrow 3_{13}$	9/2←7/2	340 798.42	0.02
$4_{14} \leftarrow 3_{13}$	7/2←5/2	341 685.04	0.02
$4_{13} \leftarrow 3_{12}$	9/2←7/2	352 204.34	0.02
$4_{13} \leftarrow 3_{12}$	7/2←5/2	352978.17	0.11
$4_{22} \leftarrow 3_{21}$	9/2←7/2	345 744.32	−0.01
$4_{22} \leftarrow 3_{21}$	7/2←5/2	348 870.95	−0.01
$4_{23} \leftarrow 3_{22}$	9/2←7/2	345 655.92	0.00
$4_{23} \leftarrow 3_{22}$	7/2←5/2	348 784.87	−0.07
$4_3 \leftarrow 3_3$ [d]	9/2←7/2	344178.34	0.01
$4_3 \leftarrow 3_3$ [d]	7/2←5/2	351 487.85	0.01
$3_{13} \leftarrow 4_{04}$	5/2←7/2	328 086.99	0.01
$3_{13} \leftarrow 4_{04}$	7/2←9/2	331 180.90	−0.03
$4_{14} \leftarrow 5_{05}$	7/2←9/2	236 364.60	0.00
$4_{14} \leftarrow 5_{05}$	9/2←11/2	238 668.93	0.00
$5_{15} \leftarrow 6_{06}$	9/2←11/2	143162.93	−0.01
$5_{15} \leftarrow 6_{06}$	11/2←13/2	144 957.34	0.06
$9_{09} \leftarrow 8_{18}$	17/2←15/2	144137.16	0.01
$9_{09} \leftarrow 8_{18}$	19/2←17/2	143190.45	0.04
$10_{0,10} \leftarrow 9_{19}$	19/2←17/2	242180.49	−0.02
$10_{0,10} \leftarrow 9_{19}$	21/2←19/2	241 420.12	−0.01
$11_{0,11} \leftarrow 10_{1,10}$	21/2←19/2	341 241.57	0.00
$11_{0,11} \leftarrow 10_{1,10}$	23/2←21/2	340634.19	0.00
$8_{26} \leftarrow 7_{17}$	15/2←13/2	2777038.60[c]	0.00

[a] Reference 13.
[b] Reference 9.
[c] Reference 11.
[d] K-type doubling is not resolved.

are, in fact, complicated combinations of constants. In recognition of this problem, attempts were made[12,14] to calculate several of the higher order constants from other sources of information such as force fields or optical data. Unfortunately, some of the constrained constants are wrong not only in magnitude, but in some cases even in sign. As a result, some very significant differences exist between earlier results and the constants of Table III. Recently, Brown, Sears, and Radford have analyzed an extensive new set of FIR LMR data,[22] with the resulting constants listed in Ref. 15. Although their results are generally similar to ours, there remain a few differences.

The inclusion of the new spin rotation centrifugal distortion term H_K^s is important to the fit. It reduces the rms deviation of the fit by approximately an order of magnitude and makes significant contributions to the spin splittings of the higher K states. It might be concluded that HCO would not require higher order spin rotation centrifugal distortion terms because ϵ_{aa} for HCO is smaller than ϵ_{aa} for HO_2. However, this conclusion does not take into account that HCO undergoes substantially more bending distortion than HO_2. This can be seen by comparing the relative sizes of Δ_K for HO_2 (~ 123 MHz) and HCO (~ 920 MHz). A careful inspection of the residuals in our earlier analysis of HO_2 reveals a small, but systematic with K splitting error. Presumably, the H_K^s is in fact required, but to a lesser degree for HO_2.

HCO occupies an intriguing position in the chemistry of interstellar molecular clouds. It is one of a class of radicals like CH and CH_2 which are thought to be formed primarily by reactions involving C^+.[23,24] As C^+ is formed efficiently by photoionization of neutral carbon, HCO and similar radicals might be expected to have reasonable abundances in regions with or near to sources of ultraviolet radiation, such as the edges of molecular clouds. The much smaller rotational constants of HCO relative to CH and CH_2 produces a correspondingly greater number of transitions accessible to astronomical receivers throughout the millimeter and submillimeter spectral region. HCO therefore currently provides the best molecular probe of the possible spatial correlation between C^+ and chemically related free radicals, as pointed out by Hollis and Churchwell[3] in their study of $N=1_{01}-0_{00}$ emission from HCO in several molecular cloud complexes.

Unfortunately, the abundance of HCO is rather low, and emission from the $N=1_{01}-0_{00}$ transition is very weak. Recent improvements in receiver performance in the millimeter wave region and the increase in line strength with frequency imply that observations of higher N transitions will substantially increase the attainable signal to noise. Indeed, it appears that Snyder *et al.*[25] have recently detected both hyperfine components of the $N=2_{02}-1_{01}$, $J=\frac{5}{2}-\frac{3}{2}$ transition. While the total dipole moment of HCO has not been measured experimentally, Landsberg *et al.*[26] have determined that $\mu_a = 1.3626(36)$ D using infrared laser electric resonance techniques. Further, Botschwina[27] has theoretically calculated that

$$\mu_a \cong 2\,\mu_b$$

at the equilibrium geometry using an unrestricted Hartree–Fock wave function. Our observations of several a and b-type transitions support this conclusion. The greater transition moments and ease of excitation in the a-type transitions below 400 GHz suggest that observations of the $4_{04}-3_{03}$ and $3_{03}-2_{02}$ transitions at 346.7 and 260.1 GHz, plus further observations of the $2_{01}-1_{01}$ transition near 173.4 GHz, offer the best hope for more detailed studies of interstellar HCO. The observations of several rotational transitions along with their fine and hyperfine components would greatly extend the usefulness of the formyl radical as a probe of the excitation mechanisms and physical conditions prevailing in the transition region between diffuse and dense molecular clouds.

TABLE III. Zero-field molecular constants (MHz) of HCO obtained in this work.

Parameter	Value (σ)	Parameter	Value (ϵ)
A	729 366.331[a]	ϵ_{aa}	11 633.879[a]
B	44 787.895[a]	ϵ_{bb}	19.032[a]
C	41 930.640[a]	ϵ_{cc}	−206.096[a]
Δ_N	0.11815(17)	ϵ_{ab}	201.0(10)
Δ_{NK}	0.455 3(16)	Δ_N^s	0.0021(5)
Δ_K	920.36(15)	Δ_{NK}^s	−0.186(17)
δ_N	0.011 90(4)	Δ_K^s	−52.93(16)
δ_K	4.59(15)	H_K^s	0.504(14)
H_{KN}	−0.013 02(16)		
a_H	388.89(12)	T_{bb}	2.57(13)
T_{aa}	11.19[b]	T_{cc}	−13.76(13)

[a]These parameters are calculated from Table IV.
[b]Calculated from T_{bb} and $T_{cc}(T_{aa}+T_{bb}+T_{cc}=0)$.

TABLE IV. Fitted linear combinations (MHz) of the rotation/spin rotation constants listed in Table III.

Parameter	Value (σ)
$A-\frac{1}{2}(B+C)$	686 007.063(160)
$\frac{1}{2}(B+C)$	43 359.268(8)
$\frac{1}{2}(B-C)$	1 428.628(580)
$-\frac{1}{3}(\epsilon_{aa}+\epsilon_{bb}+\epsilon_{cc})$	−3 815.605(19)
$-\frac{1}{6}(2\epsilon_{aa}-\epsilon_{bb}-\epsilon_{cc})$	−3 909.137(16)
$\frac{1}{2}(\epsilon_{bb}-\epsilon_{cc})$	112.564(4)

ACKNOWLEDGMENTS

The authors would like to thank Dr. Jan M. Hollis for communication of results prior to publication and Dr. Eric Herbst for useful discussions during the course of this work, which was supported by NASA Grant No. NAGW-189.

[1] P. A. Leighton, *Photochemistry of Air Pollution* (Academic, New York, 1961).

[2]L. E. Snyder, J. M. Hollis, and B. L. Ulich, Astrophys. Lett. **208**, L91 (1976).
[3]J. M. Hollis and E. Churchwell, Astrophys. J. **271**, 170 (1983).
[4]S. Saito, Astrophys. Lett. **178**, L95 (1972).
[5]A. Carrington, *Microwave Spectroscopy of Free Radicals* (Academic, London, 1974).
[6]I. C. Bowater, J. M. Brown, and A. Carrington, Proc. R. Soc. London Ser. A **333**, 265 (1973).
[7]I. C. Bowater, J. M. Brown, and A. Carrington, J. Chem. Phys. **54**, 4957 (1971).
[8]G. Herzberg and D. A. Ramsay, Proc. R. Soc. London Ser. A **233**, 34 (1955).
[9]H. M. Pickett and T. L. Boyd, Chem. Phys. Lett. **58**, 446 (1978).
[10]J. A. Austin, D. H. Levy, C. A. Gottlieb, and H. E. Radford, J. Chem. Phys. **60**, 207 (1974).
[11]J. M. Cook, K. M. Evenson, C. J. Howard, and R. F. Curl, Jr., J. Chem. Phys. **64**, 1381 (1976).
[12]J. M. Brown, J. Buttenshaw, A. Carrington, K. Dumper, and C. R. Parent, J. Mol. Spectrosc. **79**, 47 (1980).
[13]B. J. Boland, J. M. Brown, and A. Carrington, Mol. Phys. **34**, 453 (1977).
[14]B. J. Boland, J. M. Brown, A. Carrington, and A. C. Nelson, Proc. R. Soc. London Ser A. **360**, 507 (1978).
[15]J. M. Brown, K. M. Dumper, and R. S. Lowe, J. Mol. Spectrosc. **97**, 441 (1983).
[16]P. Helminger, F. C. De Lucia, and W. Gordy, Phys. Rev. Lett. **25**, 1397 (1970).
[17]F. C. Fehsenfield, K. M. Evenson, and H. P. Broida, Rev. Sci. Instrum. **36**, 294 (1965).
[18]A. Charo and F. C. De Lucia, J. Mol. Spectrosc. **94**, 426 (1982).
[19]F. C. De Lucia, R. L. Cook, P. Helminger, and W. Gordy, J. Chem. Phys. **55**, 5334 (1971).
[20]J. M. Brown and T. J. Sears, J. Mol. Spectrosc. **75**, 111 (1979).
[21]W. T. Raynes, J. Chem. Phys. **41**, 3020 (1964).
[22]J. M. Brown (private communication, 1983).
[23]T. de Jong, A. Dalgarno, and W. Boland, Astron. Astrophys. **91**, 68 (1980).
[24]A. E. Glassgold and W. D. Langer, Astrophys. J. **206**, 85 (1976).
[25]L. E. Snyder, M. Schenewerk, J. M. Hollis, and D. E. Machnik (in preparation).
[26]B. M. Landsberg, A. J. Merer, and T. Oka, J. Mol. Spectrosc. **67**, 459 (1977).
[27]P. Botschwina, Chem. Phys. Lett. **29**, 98 (1974).